Iceberg drift related to Weddell Sea ice cover

Michael P. Schodlok
Alfred-Wegener-Institute for Polar and Marine Research,
Bremerhaven, Germany

Introduction

The calving of icebergs from Antartic ice shelves and their subsequent drift cause a significant transport and input of freshwater from the ice sheet into the upper ocean. Calving events of gigantic icebergs are known to occur infrequently, but drift and life times of these giants can be easily monitored by satellite. However, a large amount of freshwater is transported away from the Antarctic icesheet through medium size and small icebergs with lengths in the order of one kilometer and less. Owing to low resolution, satellite based observations of the NIC (National Ice Center) are restricted to icebergs with a minimum length of 10 nm (1 nm = 1.852 km). Icebergs smaller than this must be tagged with buoys in order to determine their drift and decay pattern as well as their life time cycle.

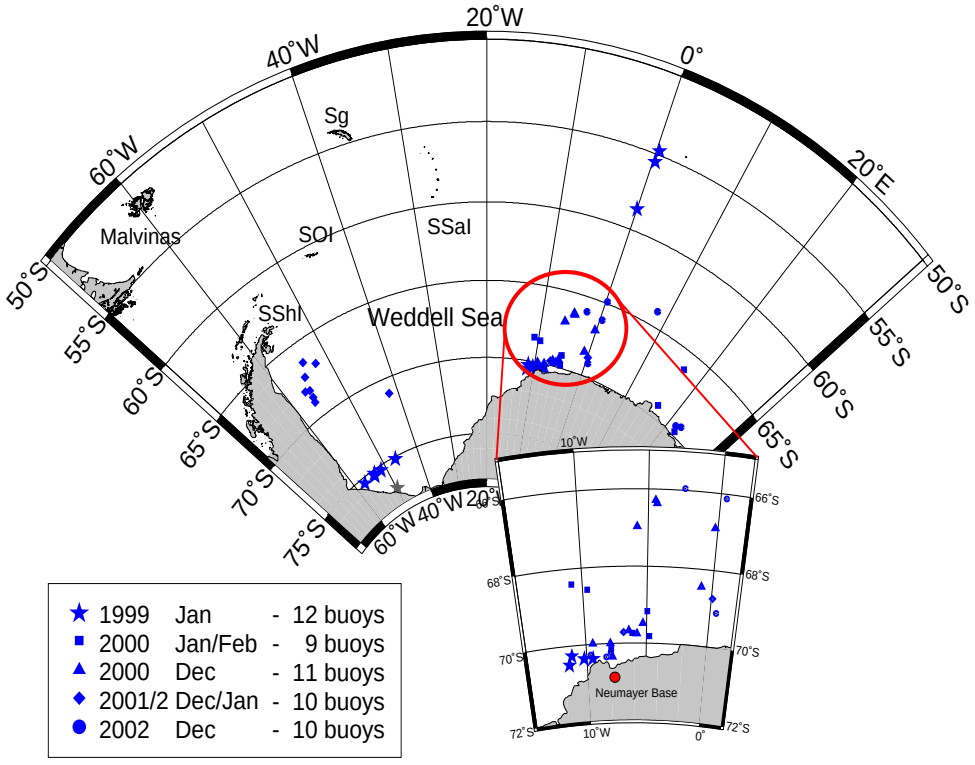

Figure 1: Deployment positions of 52 iceberg buoys tracked with the ARGOS satellite service. Abbreviations are: Sg - South Georgia, SOI - South Orkney Islands, SSaI - South Sandwich Islands, and SShI - South Shetland Islands.

From January 1999 to January 2003, 52 icebergs have been marked by the AWI with GPS sensors (some with pressure recorders) using the ARGOS satellite system to in-

vestigate propagation of small/medium sized icebergs through the Weddell Sea. The location of deployment depended on the predetermined cruise track of R/V Polarstern as well as on the availability of icebergs. Thus, as R/V Polarstern supplies Neumayer base once a year the majority of iceberg buoys were placed on icebergs in the vicinity of Atka Bay off Neumayer Base (Fig. 1 inlet). However, to cover a larger area a rather inhomogeneous distribution of these sensors was sought when possible. The buoys report their GPS positions daily at noon via the ARGOS satellite service. Since transmission and/or functionality problems result in position reports at varying time intervals, interpolation routines have to be applied. Furthermore, buoys failing to transmit over a certain amount of time are regarded as malfunctioning as they may, for example, have been crushed by ice or drowned due to iceberg capsizing. The analysis of this dataset using daily values does not allow the M_2 tide, the main component of the tidal energy in the Weddell Sea (Robertson *et al.*, 1998), to be resolved.

However, the main problem of the datasets is the use of inhomogeneously distributed buoy deployment sites, resulting in considerable variability in oceanographic and atmospheric conditions responsible for the observed iceberg drift.

This report decribes major drift patterns of certain years of deployment, investigate similarities in drift compared to sea-ice buoy data, and show iceberg movement in relation to the sea-ice cover.

Iceberg drift observations

ANT XIX/2: December 2001 - January 2002

The 2001/2002 dataset can be divided into three groups with iceberg buoys deployed a) off Neumayer Station, b) in the central southern Weddell Sea, and c) the western Weddell Sea off Larsen Ice Shelf (Fig. 1 - diamonds).

The iceberg length/width sizes vary from 50 m to 40000 m and freeboard heights from 25 to 70 m, thus drafts between 200 m and 560 m. The largest iceberg (40000 x 17000 x 50 m) marked with a buoy is probably associated with the A38 iceberg calving event in 1998. The duration of iceberg drift ranges between 340 and 460 days. It is unknown whether these short data records represents simply an instrument failure or instrument loss due, for example, to iceberg capsizing. A device to detect iceberg capsizing will be installed on future iceberg buoy sensors.

Several deployment sites were chosen to give a larger spatial coverage. However, the main focus in this paper will be on iceberg # 9367 (length = 50 m, width = 250 m, freeboard = 25 m) equipped with a buoy in the central southern Weddell Sea. Its deployment position is located at the sea-ice edge (Fig. 2). In close proximity to this iceberg three sea-ice buoys (see Kottmeier *et al.* (1997) for buoy specifications) were positioned (distance to # 8060: 62 km, # 9728: 110 km, # 9781: 145 km). Thus, a triangle of sea-ice and iceberg buoys reveals valuable information about ice deformation processes and the behaviour of the iceberg within a sea-ice field as monitored by sea-ice buoys.

All buoys were released just north of the continental shelf break closely following the continental slope on the way north (Fig. 2). The northward progression of the iceberg through/with the sea-ice field can be separated in three sections. The southern part from January to the end of March (Julian day 90) shows a velocity of 6 $\pm$ 4 km/day in a sea-ice cover of 68 $\pm$ 16 % ice concentration. From April to mid June the drift velocities within a mean sea-ice cover of 97 $\pm$ 3 % amounts to 12.2 $\pm$ 7.5 km/day, and from mid June to the end of the record the drift, with a stronger eastward velocity component, shows a mean progress of 17.5 $\pm$ 10.7 km/day. It is notable that the overall eastward transfer starts at day 175, when the tracks cross the southern extension of the Endurance Ridge. This latter feature is seen in iceberg as well as sea-ice buoy motion. From 1 April to Mid June iceberg and sea-ice motion are in very good agreement.

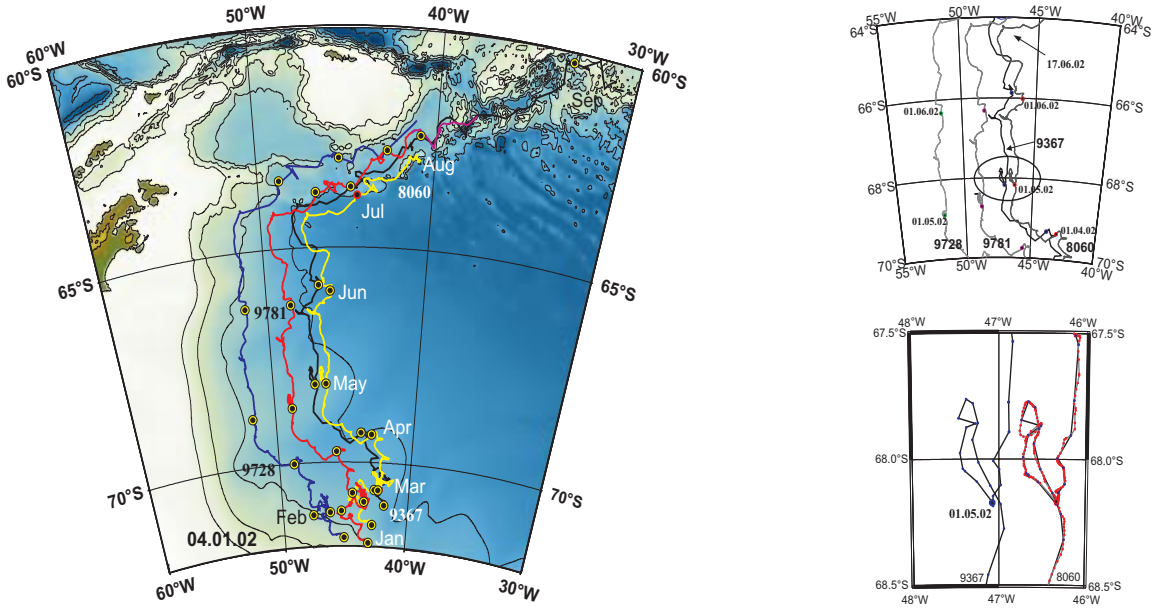

Figure 2: Left: Drift pattern of iceberg # 9367 and sea-ice buoys # 8060, # 9781, and # 9728 from point of deployment in January 2002 to August 2002. Whereas iceberg data are available till September, sea-ice buoy data are rather dubious from August. The bottom topography is derived from the GEBCO 1-min (GEBCO, 2003) data set with isopleths shown at 1000 m intervals. Right: Iceberg and sea-ice buoy drift patterns from April to July 2002 (top). Comparison between iceberg path (# 9367) with 24-h sampling interval and sea-ice buoy # 8060 with 3-h sampling interval for the circled area in top panel. The black track beneath represents the daily sea-ice buoy position at noon matching the iceberg position recording time (bottom).

The drift velocities south of 70°S compare well with the iceberg motion determined by Vinje (1980) along 40°W. The overall northward drift pattern is interrupted by two anticyclonic features, the first starting on 17 April and taking 14 days to complete the cycle, and the second starting on 20 May lasting for 4 to 7 days (Fig. 2 right). These features, causing a relatively low mean northward movement at the beginning of the drift show a predominant behaviour as the amplitude of northward extent decreases towards the west. In fact, sea-ice motion deduced by sea-ice buoy positions reveal a similar mean progression for the period April to mid June, decreasing slightly towards the west (# 8060 11.6 $\pm$ 7.6 km/day; # 9781 10.6 $\pm$ 7.3 km/day, and # 9728 9.8 $\pm$ 7.6 km/day). It is remarkable how coherent the drift patterns of sea-ice buoy # 8060 and

the iceberg, are though the distance to the iceberg varies by about 34 $\pm$ 6 km during this period and is much larger before that.

As an example of atmospheric conditions along the drift trajectories the air temperature at buoy # 9781 reveals the seasonal cycle with lowest temperatures in austral winter (Figure 3). However, as the buoy ensemble drifts northward the minimum temperature increases compared to lowest temperatures in May and June . Temperatures are well below the freezing point of the ocean and thus melting of sea-ice does not occur for the entire drift period. Towards the northern part of the drift warm temperature intrusions occur about every 4 days, related to passing low pressure systems (King and Turner, 1997).

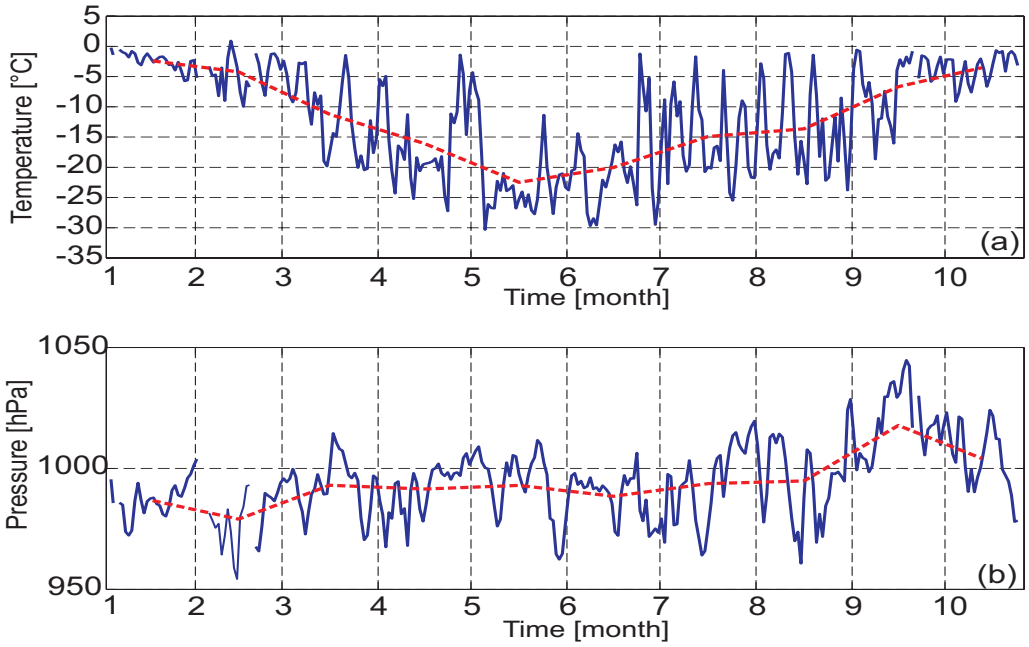

Figure 3: a) Temperature vs time and b) pressure vs time for buoy # 9781 close to iceberg # 9367 resembling atmospheric conditions during the drift through the western Weddell Sea. The solid lines are daily, dashed lines monthly mean values.

The sea-ice concentration is derived from SSM/I data using the 85 GHz channel which provides a resolution of around 15 x 13 km (Kaleschke *et al.*, 2001; Kern and Kaleschke, 2002). The analysis of sea-ice concentration at the locations of the iceberg and the sea-ice buoys indicates that for 100 % sea-ice concentration a mechanical link between the drifters exist due to a closed ice cover, despite their being about 30 km apart. The sea-ice cover, as indicated in Figs. 4 (a-c), grows from the beginning of buoy deployment (April) to the end of the record (September), the time of maximum sea-ice extent. At that time the drift ensemble reaches the nothern ice edge or the west wind zone. Whilst ice concentrations at the buoys vary at the beginning of the drift between 50 and 80 %, starting at day 87 the ice concentration is above 90 % until the ensemble reaches the northern Weddell Sea off Joinville Island. In fact, from April to mid June the sea-ice concentration at all 4 buoys is above 97 %. Thus, a high sea-ice concentration seems necessary for a coherent iceberg sea-ice motion as proposed by Lichey and Hellmer (2001) in their modelling studies of iceberg drift.

Iceberg drift trajectories showing a coherent northward motion pattern were found in two further data sets, during cruises ANTXVII/2 (January 2000) and ANTXVIII/3 (December 2000). The 90 % ice concentration threshold for coherent iceberg motions holds for icebergs equipped with buoys during ANTXVII/2 (above 92 %) but is less pronounced for those equipped during ANTXVIII/3 (decreasing sea-ice concentration from the onset of coherent iceberg motion - mean ice concentration of around 83 %). The latter might be due to the fact that the icebergs are close to the ice edge which were not well resolved by satellite data. Furthermore, direct observations of sea-ice motion is not available during these two cruises as sea-ice buoy data does not exist.

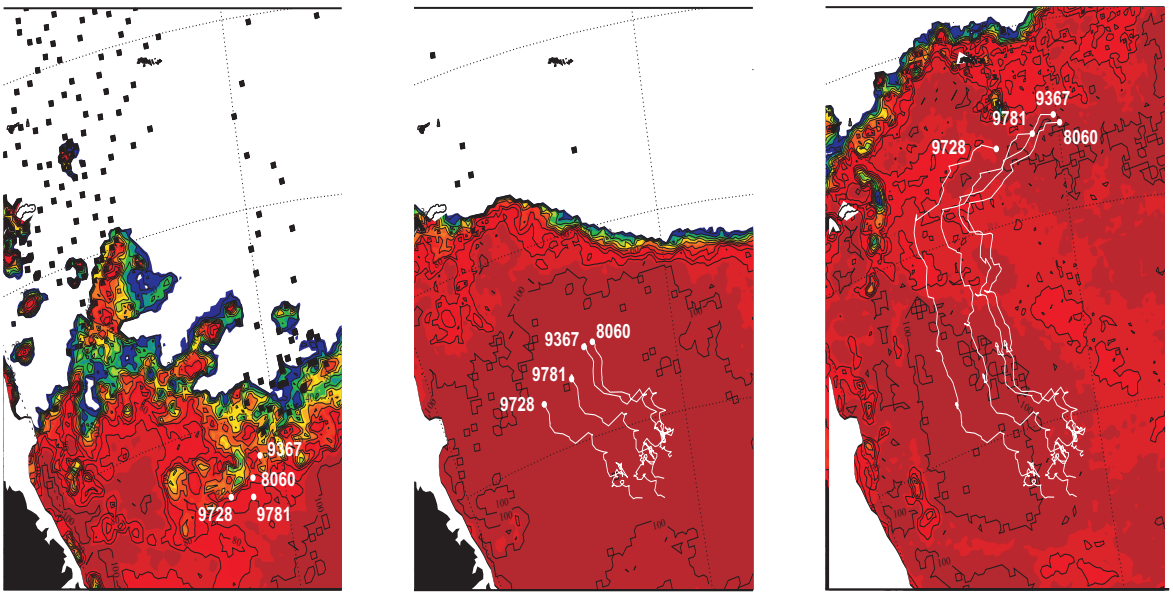

Figure 4: Left: iceberg sea-ice buoy ensemble 04.01.2002 day of deployment. Mid: iceberg sea-ice buoy ensemble 04.04.2002. Right: iceberg sea-ice buoy ensemble 04.06.2002.

Conclusion

The long-term motion of sea-ice and icebergs agrees with the circulation of the Weddell Gyre. Only during northerly winds is the general drift temporarily reversed as also shown by Thomas *et al.* (1995). Shorter time scales such as tidal motion are not resolved with the current iceberg/buoy record. However, the buoy-iceberg array might well be within the limits of a length scale in which coherent motion of the sea-ice cover occurs; in the Arctic Ocean this length scale is proposed to be 400 km (Thorndike, 1986).

The conformity in northward motion is due to the steering influence of the highly consolidated sea-ice cover, movement of which is controlled by the wind. The proposed sea-ice concentration threshold of 90 % being necessary for capturing icebergs in large scale ice fields (Lichey and Hellmer, 2001) was confirmed by these observations. The westward decrease of the northward movement might be due to the transition to ice regimes influenced by shore fast ice with increasing mechanical friction

forces.

For future studies, sea-ice iceberg buoy arrays are needed associated with a higher temporal position transmission rate in order to demonstrate whether the 90 % threshold assumption is appropriate for all Weddell Sea areas. The effects of waves as well as of tides need to be taken into account by adding more sensors, including strain and tilt sensors, to the iceberg buoy for a better understanding of the iceberg decay. The latter is essential for determining a significant component of the Southern Ocean freshwater budget.

References

GEBCO (2003). Centenary Edition of the GEBCO Digital Atlas. published on CD-ROM on behalf of the IOC and IHO as part of the General Batymetric Chart of the Oceans, BOCD, Liverpool.

Kaleschke, L., Heygster, G., Lüpkes, C., Borchert, A., Hartmann, J., Haarpainter, J., and Vihma, T. (2001). SSM/I sea ice remote sensing for mesoscale Ocean-Atmosphere interaction analysis. *Can. J. Rem. Sens.*, **27**, 526–537.

Kern, A. and Kaleschke, L. (2002). Two ice concentration algorithms benefitting from 85Ghz Special Sensor Microwave/Imager data: A comparison. *submitted to IGARSS02*.

King, J. C. and Turner, J. (1997). *Antarctic meteorology and climatology*. Cambridge University Press.

Kottmeier, C., Ackley, S., Andreas, E., Crane, D., Hoeber, H., King, J., und D. Limbert, J. L., Martinson, D., Roth, R., Sellmann, L., Wadhams, P., and Vihma, T. (1997). Wind, temperature and ice motion statistics in the Weddell Sea. *WMO/TD*, **979**, 48.

Lichey, C. and Hellmer, H. H. (2001). Modeling giant iceberg drift under the influence of sea ice in the Weddell Sea. *J. Glaciol.*, **47**, 452–460.

Robertson, R. L., Padman, L., and Egbert, G. D. (1998). Tides in the Weddell Sea. In S.S. Jacobs and R.F. Weiss, editor, *Ocean, Ice and Atmosphere: Interactions at the Antarctic Contin ental Margin*, volume **75** of *Antarc. Res. Ser.*, pages 341–369. AGU.

Thomas, J. P., Turner, J., Lachlan-Cope, T. A., and Corcoran, G. (1995). High resolution observations of Weddell Sea surface currents using ERS-1 SAR sea-ice motion vectors. *Int. J. Remote Sensing*, **16**, 3409–3425.

Thorndike, A. S. (1986). Kinematics of sea ice. In N. Untersteiner, editor, *The geophysics of sea ice*, volume **146** of *NATO ASI Series B: Physics*, pages 489–550. Plenum Press, New York.

Vinje, T. E. (1980). Some satellite-tracked iceberg drifts in the Antarctic. *Annals of Glaciology*, **1**, 83–87.